Thermochimica Acta, 116 (1987) 71–77
Elsevier Science Publishers B.V., Amsterdam – Printed in The Netherlands

STUDY OF AUC THERMAL DECOMPOSITION KINETICS IN NITROGEN BY A NON-ISOTHERMAL METHOD

GE QINGREN and KANG SHIFANG

Department of Chemical Engineering, Tianjin University, Tianjin (China)

(Received 27 October 1986)

ABSTRACT

The thermal decomposition kinetics of AUC (ammonium uranyl carbonate) in nitrogen have been determined by a non-isothermal method. DSC curves are solved by computer with a non-linear fitting method. The results show that the particle size has no apparent influence on decomposition rate, and the kinetics obey the Avrami–Erofeev equation within 90% conversion. The apparent activation energy and pre-exponent are found to be 105.5 kJ mol^{-1} and 2.17×10^{10} s^{-1}, respectively.

INTRODUCTION

AUC (ammonium uranyl carbonate) is an important intermediate product in the nuclear fuel cycle. In comparison with other processes, the AUC process has the following advantages: (a) purification during the process of crystallization is good and (b) uranium dioxide obtained from AUC has better reactivity [1], and better characteristics of powder for producing reactor elements [2].

Thermal decomposition is one of the key processes in AUC conversion. The intermediate phases, when AUC is reduced to UO_2, had been studied by TG, DSC, EM, X-ray and electron diffraction [3,4]. The investigation of AUC decomposition kinetics has not yet been reported in detail in the published literature. The decomposition of AUC is an intense endothermal reaction, $\Delta H_{298} = 510.8$ kJ mol^{-1} [5,6], which will aggravate the defect of the "zero time" effect of the isothermal thermogravimetric method. Because of this the non-isothermal calorimetric method is used in the present work.

EXPERIMENTAL

The AUC sample (nuclear purity grade) used in the experiments was obtained from nuclear fuel works and dried in air at room temperature, then stored in a sealed container until use. AUC decomposition kinetics were determined with a CDR-1 type DSC made in the Shanghai Balance Factory.

0040-6031/87/$03.50

The runs were carried out in dry nitrogen with a flow rate of 100 cm^3 min^{-1} under heating rates of 1, 2, 5 and 10 °C min^{-1}, and a sample mass of 3–5 mg of α-Al_2O_3 was used as the reference sample in the experiments. The cross section and morphology of the sample were observed and photographed with DRC-1 type stereo microscope made by the German Opton Company.

DATA TREATMENT

Determination of apparent activation energy by the Kissinger method

For solving apparent activation energy from non-isothermal kinetics curves, Kissinger [7] proposed the following working equation:

$$\frac{\mathrm{d}\ \ln\left(\beta/\mathrm{R}T_\mathrm{m}^2\right)}{\mathrm{d}(1/T_\mathrm{m})} = -E/\mathrm{R} \tag{1}$$

where β is the heating rate, R the gas constant, E the apparent activation energy and T_m the peak temperature of the DSC curve. A straight line can be obtained by plotting $\ln(\beta/\mathrm{R}T_\mathrm{m}^2)$ against $1/T_\mathrm{m}$ from a set of DSC curves at different heating rates, and the apparent activation energy is calculated from the slope of the straight line.

Determination of apparent activation energy by the Ozawa method

Using the Doyle approximation equation, Ozawa [8] derived the working equation as follows:

$$\frac{\mathrm{d}\ \log \beta}{\mathrm{d}(1/T)} = -0.4567E/\mathrm{R} \tag{2}$$

where T is the temperature corresponding to a certain conversion in a set of the kinetics curves.

Solving non-isothermal kinetics curves by a non-linear fitting method [9]

Based on the fact that the absorbed heat in the reaction is directly proportional to AUC decomposition quantity, the height of the DSC curves from the base line is proportional to the decomposition rate and the area under the DSC curves is proportional to the decomposition conversion. The peak area of the DSC curves can be measured by the paper-cutting weight method or by Simpson's integration method. Both methods give similar results.

The DSC curves of AUC decomposition, determined at different heating rates, are converted into the integration kinetics curves by the above-men-

TABLE 1

Conversion functions of different mechanisms

Mechanism	Conversion function $g(\alpha)$
Internal diffusion (two dimensions)	$(1-\alpha)\ln(1-\alpha)+\alpha$
Internal diffusion (three dimensions)	$1-3(1-\alpha)^{2/3}+2(1-\alpha)$
Chemical reaction (two dimensions)	$1-(1-\alpha)^{1/2}$
Chemical reaction (three dimensions)	$1-(1-\alpha)^{1/3}$
Nucluation and nuclei growth	$-\ln(1-\alpha)$
Nucleation and nuclei growth	$[-\ln(1-\alpha)]^{2/3}$
Nucleation and nuclei growth	$[-\ln(1-\alpha)]^{1/2}$
Nucleation and nuclei growth	$[-\ln(1-\alpha)]^{1/3}$
Nucleation and nuclei growth	$[-\ln(1-\alpha)]^{1/4}$

tioned method, then the required data are taken at intervals on the integration kinetics curves and substituted into the following iterative equation:

$$E_n = \frac{RT_{m+n}T_n}{T_{m+n}-T_n}\left\{\ln\left[\left(\frac{RT_n}{E_n}\right)^2 - 2\left(\frac{RT_n}{E_n}\right)^3 + 6\left(\frac{RT_n}{E_n}\right)^4\right] - \ln\left[\left(\frac{RT_{m+n}}{E_n}\right)^2 - 2\left(\frac{RT_{m+n}}{E_n}\right)^3 + 6\left(\frac{RT_{m+n}}{E_n}\right)^4\right] + \ln\left[\frac{g(\alpha_{m+n})-g(\alpha_0)}{g(\alpha_n)-g(\alpha_0)}\right]\right\} \tag{3}$$

where n is the ordinal number, m the interval number, $g(\alpha)$ the conversion function of different mechanism and α_0 the initial conversion of the AUC sample. This paper uses nine kinds of mechanism function listed in Table 1 to fit the experiment curves.

The initial value of E is taken to be 840 kJ mol^{-1} to solve the iterative equation, and the convergent requirement is less than 10^{-3} kJ mol^{-1}.

To solve the preexponent, Z_n, E_n, solved from Eqn. (3), substitute the following equation:

$$Z_n = \frac{R\beta}{E_n}\exp\left\{\frac{RT_n}{E_n} - \ln\left[\left(\frac{RT_n}{E_n}\right)^2 - 2\left(\frac{RT_n}{E_n}\right)^3 + 6\left(\frac{RT_n}{E_n}\right)^4\right] + \ln[g(\alpha_n)-g(\alpha_0)]\right\} \tag{4}$$

Values of E_n and Z_n are calculated for every mechanism, respectively. To obtain the fitting curves, E_n and Z_n of different mechanisms, substitute the following equation:

$$X = \ln\left(\frac{1!}{X^2} - \frac{2!}{X^3} + \frac{3!}{X^4}\right) + \ln\left(\frac{ZE}{R\beta}\right) - \ln[g(\alpha)-g(\alpha_0)] \tag{5}$$

$$X = \frac{E}{RT} \tag{6}$$

The fitting curves of nine kinds of mechanism will be obtained and compared with kinetics curves determined experimentally to obtain the fitting error calculated by the least squares method. The solutions required are obtained by using both the criteria of least fitting error and the apparent activation energy determind by Kissinger's or Ozawa's method. All computational processes are carried out on a 441-B type computer.

RESULTS AND DISCUSSION

DSC curves of the decomposition of the AUC sample with different particle sizes at different heating rates in nitrogen are determined. According to the principle of the absorbed heat being directly proportional to the conversion of reaction, DSC curves are converted into correlation curves between conversion and temperature. Typical curves are shown in Fig. 1.

From Fig. 1, it is seen that the position of the kinetics curve moves to higher temperature with the increase of heating rate. The decomposition of AUC starts about 100 °C and conversion at inflection of the curves is about 60%. Other non-isothermal kinetics curves of different particle sizes are essentially identical and are not shown here.

The apparent activation energy of AUC decomposition, E_k and $\bar{E}_0$, are determined by Kissinger's and Ozawa's methods. Typical plots are shown in Figs. 2 and 3. The results show that both methods give approximate values.

Taking E_k and fitting error as criteria, the non-isothermal kinetics curves are solved by the above-mentioned method. The results obtained are shown in Table 2. From Table 2, it is seen that all the decomposition kinetics of the

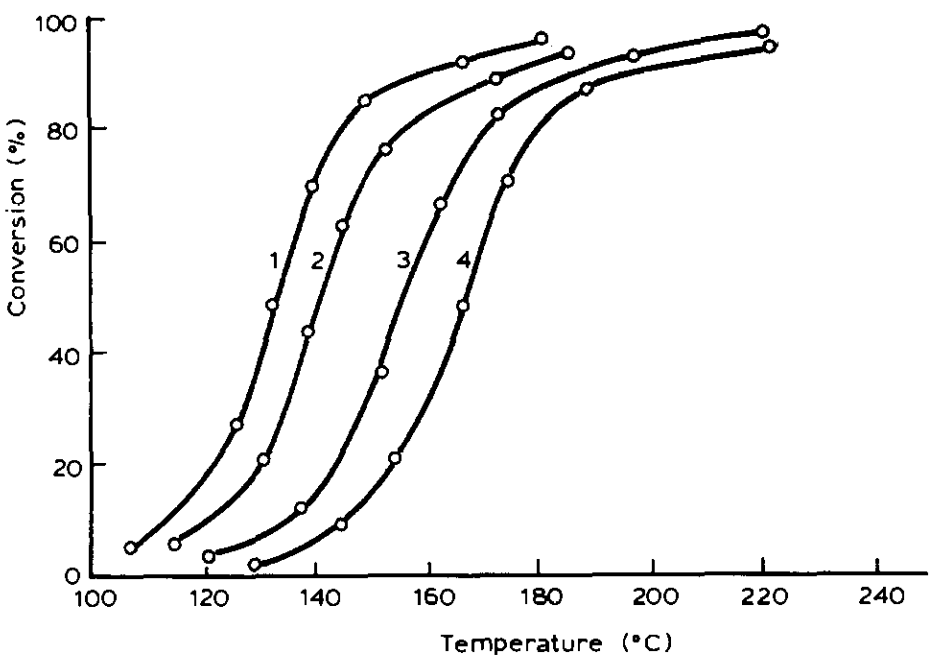

Fig. 1. Non-isothermal kinetic curves of AUC decomposition: Heating rate (1) 0.9 °C min^{-1}; (2) 1.8 °C min^{-1}; (3) 4.5 °C min^{-1}; (4) 9.1 °C min^{-1}. Atmosphere, N_2; particle size, $-320+360$ mesh.

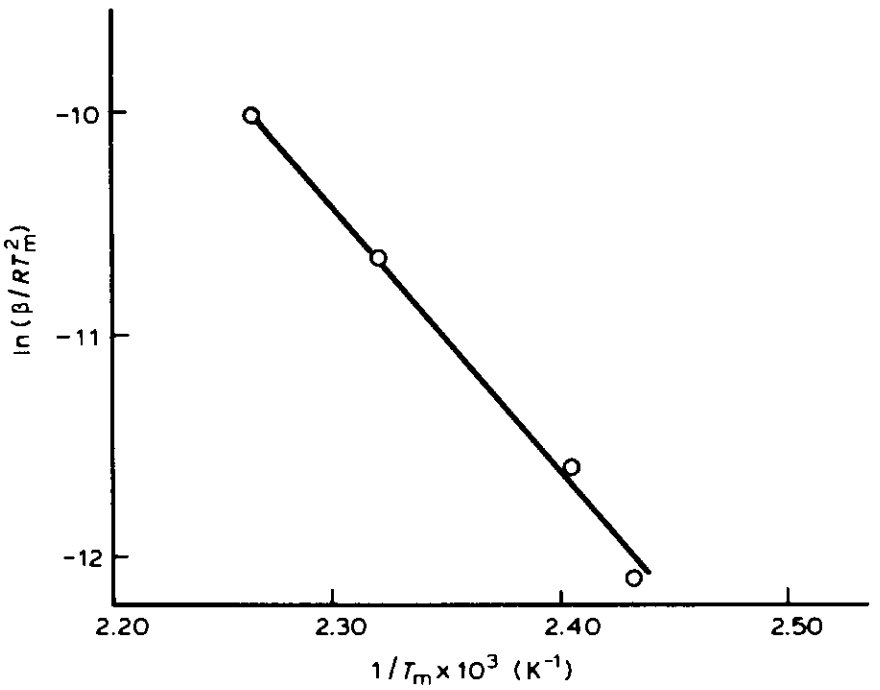

Fig. 2. Kissinger plot of AUC decomposition. Atmosphere, N_2; particle size, $-320+360$ mesh; $E_k = 98.0$ kJ mol^{-1}.

AUC samples with different particle sizes and also the unsieved AUC sample in nitrogen within 90% conversion obey the Avrami-Erofeev equation:

$$[-\ln(1-\alpha)]^{2/3} = Z \exp(-E/RT)t \tag{7}$$

or

$$\frac{d\alpha}{dt} = \tfrac{3}{2}(1-\alpha)[-\ln(1-\alpha)]^{1/3} Z \exp(-E/RT) \tag{8}$$

where E is the apparent activation energy and Z the pre-exponent. The

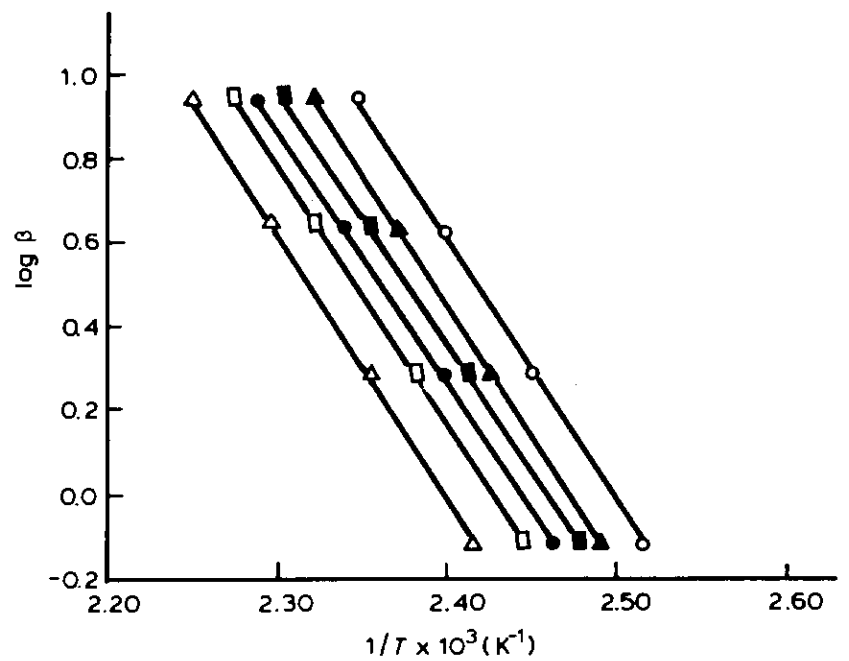

Fig. 3. Ozawa plot of AUC decomposition: (○) 20% conversion; (▲) 30% conversion; (■) 40% conversion; (●) 50% conversion; (□) 60% conversion; (△) 70% conversion. Atmosphere, N_2; particle size, $-320+360$ mesh; $\bar{E}_0 = 94.6$ kJ mol^{-1}

TABLE 2

Solutions of non-isothermal kinetics curves of AUC decomposition

Particle size of AUC (mesh)	Heating rate (°C min^{-1})	Conversion function (g (α))	Apparent activation energy (kJ mol^{-1})	ln Z (s^{-1})	Fitting error[a] (°C)
−320+360	0.9	$[-\ln(1-\alpha)]^{2/3}$	98.8	22.0	2.9
−320+360	1.8	$[-\ln(1-\alpha)]^{2/3}$	100.5	22.8	1.7
−320+360	9.1	$[-\ln(1-\alpha)]^{2/3}$	112.2	25.8	2.2
−160+200	1.9	$[-\ln(1-\alpha)]^{2/3}$	109.7	25.2	1.4
−160+200	9.3	$[-\ln(1-\alpha)]^{2/3}$	107.2	24.5	1.2
−80+100	0.9	$[-\ln(1-\alpha)]^{2/3}$	107.6	24.4	2.2
−80+100	1.8	$[-\ln(1-\alpha)]^{2/3}$	102.6	23.0	2.1
−80+100	4.6	$[-\ln(1-\alpha)]^{2/3}$	103.8	23.0	1.9
−80+100	9.2	$[-\ln(1-\alpha)]^{2/3}$	103.4	23.1	1.4
Unsieved	4.5	$[-\ln(1-\alpha)]^{2/3}$	103.4	23.2	0.9
Unsieved	9.1	$[-\ln(1-\alpha)]^{2/3}$	104.3	23.4	2.2

[a] The standard deviation between fitting and kinetics curves determined experimentally.

average value of E is 105.5 kJ mol^{-1} and the average value of Z is 2.7×10^{10} s^{-1}.

For further verification, the cross sections of particles have been observed. AUC samples of partial decomposition solidify in plastic and the specimen is polished, then observed and photographed with a microscope (cf. Fig. 4).

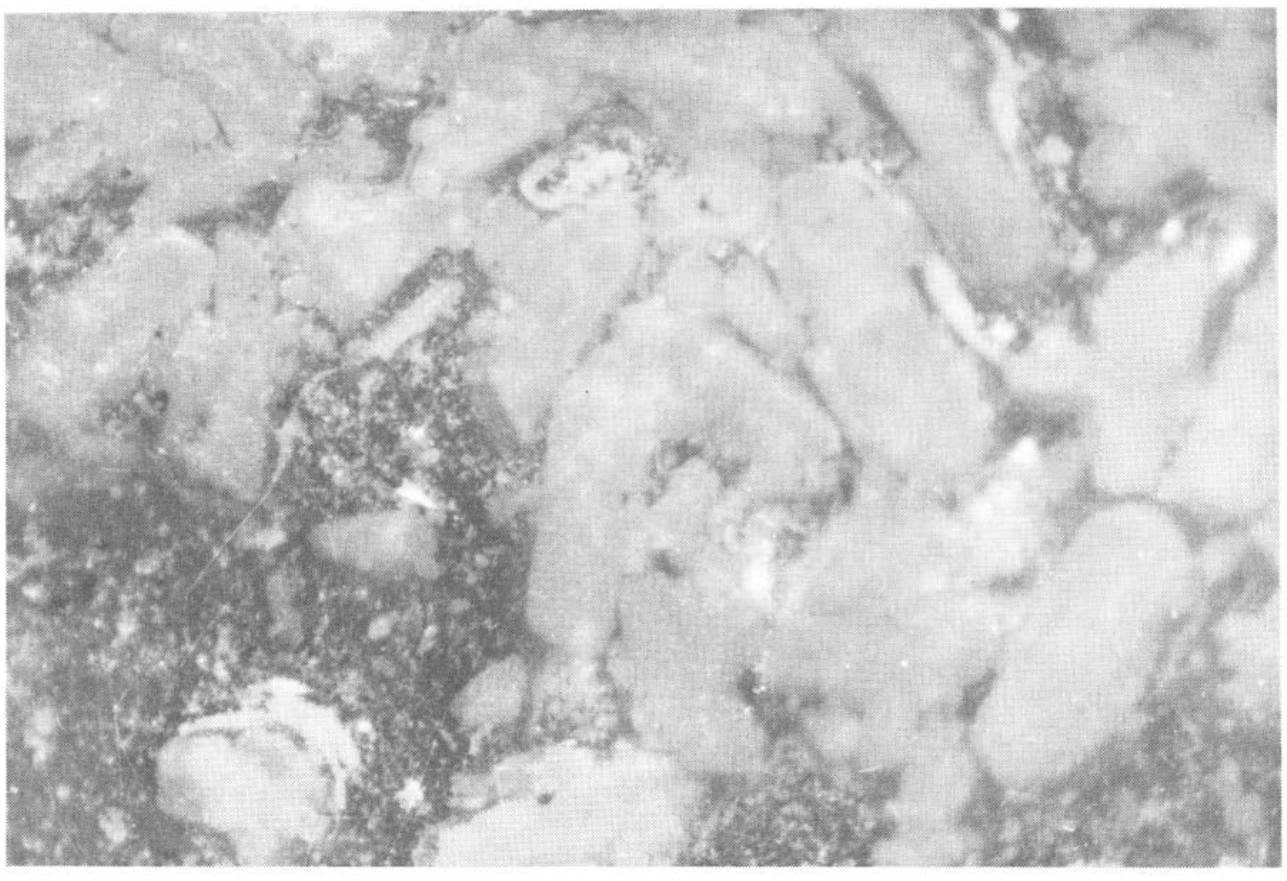

Fig. 4. Micrograph of the cross section of an AUC particle of partial decomposition (45% conversion).

It is shown that AUC decomposition occurs uniformly within the particle and the sharp interface of orange UO_3 and yellow AUC is not found. This observation agrees with the mechanism controlled by the nucleation of new phase and the growth of nuclei, since the nucleation and the growth of nuclei during the reaction are random in either time or space and every local equivalent fragment is equal, according to the Avrami–Erofeev mechanism [10].

REFERENCES

1 Q.R. Ge, S.F. Kang, C. Shang and P.J. Cong, Chinese J. Nucl. Sci. Eng., 2 (1982) 43.
2 H. Assmann and M. Becker, Trans. Am. Nucl. Soc., 31 (1979) 147.
3 L. Halldahl, J. Nucl. Mater., 126 (1984) 170.
4 L. Halldahl and Nygren, Thermochim. Acta, 72 (1984) 213.
5 H.G. Bachmann, J. Inorg. Nucl. Chem., 37 (1975) 735.
6 Q.R. Ge and C. Shang, unpublished work.
7 H.E. Kissinger, Anal.Chem., 29 (1957) 1702.
8 T. Ozawa, Bull. Chem. Soc. Jpn., 38 (1965) 1881.
9 Q.R. Ge, unpublished work.
10 N.B. Hanney, Treatise on Solid State Chemistry, Vol. 4, Plenum Press, New York, 1976, Chap. 4.